Journal of South American Earth Sciences 106 (2021) 102869

Contents lists available at ScienceDirect

Journal of South American Earth Sciences

journal homepage: www.elsevier.com/locate/jsames

New paleomagnetic data from the Paraná Magmatic Province: Brief emplacement time and tectonism

Marcia Ernesto [a,*], Luiz Alberto Zaffani [a,b], George Caminha-Maciel [c]

[a] Universidade de São Paulo, Instituto de Astronomia, Geofísica e Ciências Atmosféricas, Departamento de Geofísica, 05508-900, São Paulo, SP, Brazil
[b] Universidade Metropolitana de Santos, Brazil
[c] Universidade Federal de Santa Catarina, Departamento de Geologia, Florianópolis, SC, Brazil

ARTICLE INFO

Keywords:
Paraná magmatic province
Paleomagnetism
Early Cretaceous
Intraplate deformation

ABSTRACT

The Paraná Magmatic Province (PMP) in southern Brazil is divided into three sub-provinces historically characterized by their Ti content (low-Ti in the southern sub-province, high-Ti in the northern, and mixed in the central sub-province). Ar/Ar and U-Pb ages for the PMP usually places the whole volcanism in a brief interval of ~135-133 Ma with younger ages to the north. The existing paleomagnetic data tend to show differences among the three areas, so far related to the age migration. The new data from 39 flows and sills from the Northern Paraná Magmatic Province incorporated into the pre-existing database allowed the calculation of a new paleomagnetic pole after filtering the over-represented sites. However, the recalculated pole for the central PMP using all available data is distinct from the other poles. The mean magnetic inclination for the rocks of central PMP is ~5° lower than the inclination for the other areas, which may be caused by an N-S dipping of the central area.

1. Introduction

The Paraná Magmatic Province (PMP, Fig. 1) represents one of the most remarkable Phanerozoic flood basalt events in the world (Piccirillo and Melfi, 1988; Milani et al., 2007), which led to the rupture of the Western Gondwana during the Early Cretaceous. The PMP volcanic rocks cover all southern Brazil and parts of Uruguay, Argentina, and Paraguay. In pre-drift reconstructions, the Etendeka magmatism in Namibia, Africa, is contiguous to the PMP, and therefore the entire province is designated as the Paraná-Etendeka Province.

A high number of good quality radiometric ages based on the Ar/Ar method (Renne et al., 1992, 1996; Turner et al., 1994; Stewart et al., 1996; Ernesto et al., 1999; Mincato et al., 2003) indicate that PMP activity was initiated in the south near the Hauterivian stage and continued northward. In this region, Barremian intrusive equivalents are exposed. The available ages were recalculated according to modern standards (Thiede and Vasconcelos, 2010; Janasi et al., 2011) and confirmed the hypothesis of a rapid (1–3 Ma) emplacement of the whole province. An age of 135 ± 1 Ma for the south part of the PMP and continuing northwards up to ~133 Ma with the injection of the Ponta Grossa dike swarm. A U-Pb baddeleyite/zircon of 134.3 ± 0.8 Ma reported for dacites from the Ponta Grossa area (Janasi et al., 2011) is in general agreement with the PMP history. This temporal model fits the paleomagnetic data (Ernesto et al., 1990) from the south and north areas. However, Dodd et al. (2015) claim that the Paraná-Etendeka Province must span a longer time interval (>4 Ma) as the authors identified various polarity zones within the magnetostratigraphic record. The PMP sections also show multiple polarity zones (Ernesto et al., 1990). However, due to the high reversal frequency of the geomagnetic field during Lower Cretaceous, this fact is not in disagreement with the thesis of a rapid emplacement. Furthermore, extemporary intrusive magmatic activity (Hartmann et al., 2019) indicates that the volcanism extended beyond the narrow time interval advocated for the main igneous phase.

Significant chemical differences also characterize the PMP basalts, particularly the content of Ti and the incompatible elements. The low-Ti rocks are found in the south, and the high-Ti rocks are in the north. However, in between these two areas, the so-called central PMP (CPMP) delimited by the Rio Uruguay and the Rio Piquiri lineaments (Fig. 1), both chemical types are found. In the PMP, there exist two types of acid rocks - the Palmas type in the south and central areas, and the Chapecó type in the central and north regions (Piccirillo and Melfi, 1988). Sills and dikes are also abundant, mainly on the northeastern border of the PMP. They have the same chemical characteristics and similar ages as

* Corresponding author.
E-mail addresses: mernesto@usp.br (M. Ernesto), thezaffani@yahoo.com.br (L.A. Zaffani), caminha.maciel@ufsc.br (G. Caminha-Maciel).

https://doi.org/10.1016/j.jsames.2020.102869
Received 18 April 2020; Received in revised form 19 August 2020; Accepted 29 August 2020
Available online 4 September 2020

the basalts of the north PMP (NPMP; Ernesto et al., 1999; Machado et al., 2015).

In the reconstructions of the Western Gondwana, the best fit between South America and Africa is achieved by producing some internal deformation of the South American plate (Moulin et al., 2010). As the PMP preceded the South Atlantic opening, it may be affected by the proposed intracontinental transcurrences (Curie, 1984; Unternher et al., 1988; Moulin et al., 2010). Curie (1984) suggested a transcurrent movement through the Paraná Basin, as a continuation of the Walvis-São Paulo chains. Conceição et al. (1988) claimed for a discontinuity along the NW-oriented Curitiba-Maringá shear zone related to the Ponta Grossa Arch. Chang et al. (1992) questioned these models as they lack geological and geophysical pieces of evidence. In contrast, the authors proposed a model that involves strain accommodation through the rotation of South America about Africa, producing an extension in the NE-SW direction and injection of NW-SE trending dikes. However, the paleomagnetic data used in plate reconstructions are systematically corrected to intraplate tectonics since the work of Schetino and Scotese (2005).

Paleomagnetism is the best tool to investigate lithospheric/crustal deformations, providing that they involve block rotation or latitude variation. Another condition is that the paleomagnetic data sets used in the detection of the tectonic deformation are large enough and reliable to overcome the influences of the geomagnetic time variations. The paleomagnetic database for the PMP has been enlarged in the last decade with data from different regions: northeastern region of the basin (Ernesto et al., 1999), central region (Alva-Valdivia et al., 2003) Paraguay (Ernesto et al., 1996; Goguitchaichvili et al., 2013) and Argentina (Mena et al., 2006). However, in the north area, data are still scarce, and most of the available results come from the sills in the eastern border. In this work, we present a set of new data from the northern PMP to provide a reliable comparison between the two areas of the province and to check if there is any evidence of significant intra-continental movements affecting the PMP.

2. Geological outlines and sampling

The PMP is characterized by voluminous accumulations of flood basalts that covered the Paraná sedimentary basin. Sedimentation in this basin started in the Early Paleozoic and ended in the Late Jurassic/Early

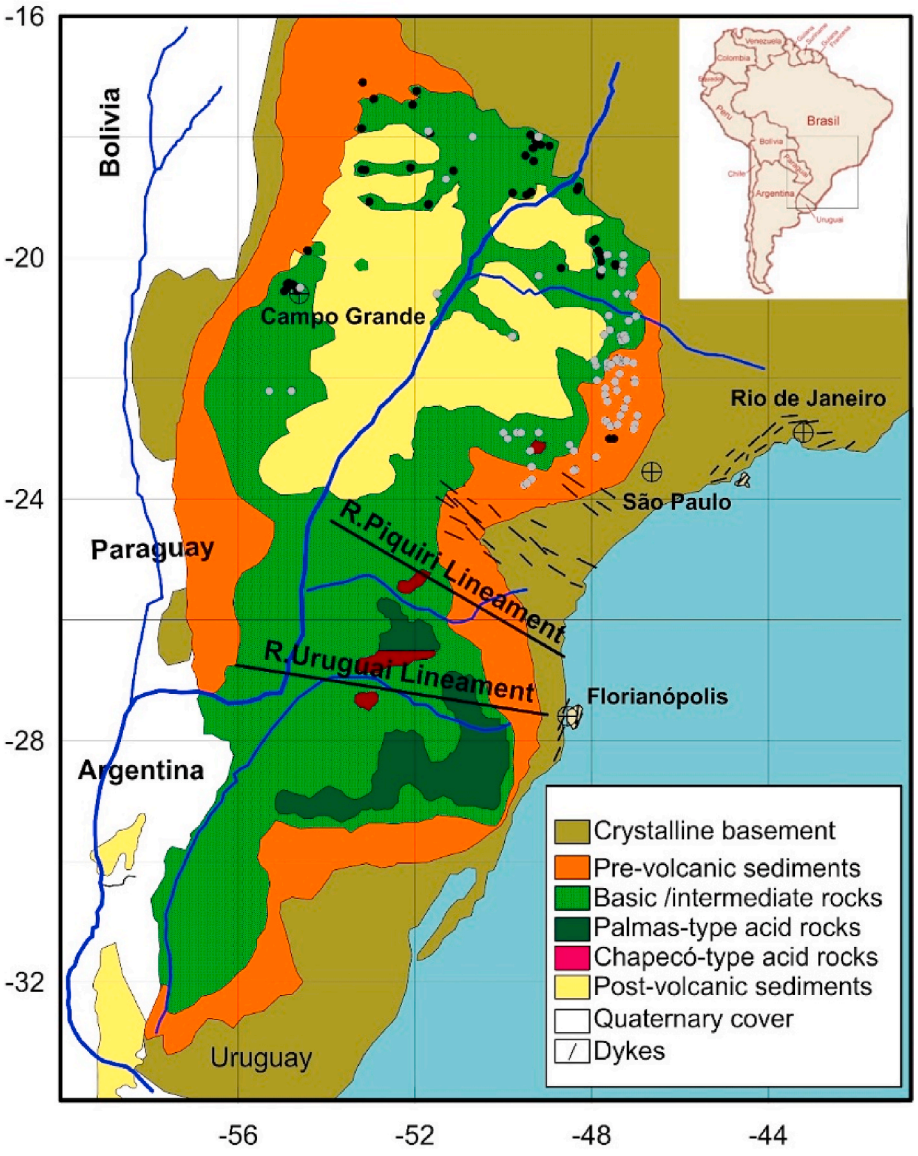

Fig. 1. Simplified geologic map of the Paraná Magmatic Province and the sampling sites (black dots) analyzed in this work, along with the previously studied sites (light dots) from NPMP.

Cretaceous with the aeolic deposits of the Botucatu Formation. The Paraná basalts overlay the aeolic Botucatu sandstones. However, in the northeast area of the PMP, the basalts may lay directly over the crystalline basement (Petri and Fulfaro, 1983).

The best exposures of the PMP successions are in the escarpments of the southern area (SPMP; south of the Rio Uruguai lineament; Fig. 1). Up to 1,100 m of lavas are exposed along several roadcuts. However, a maximum thickness of 1,700 m was reported by Almeida (1986) in the north PMP (NPMP), although the flatter relief in the area exposes only the upper part of the sequences. In the NPMP, acidic rocks (about 3% in volume) are rare but sometimes found laying directly on the Botucatu sediments (Piccirillo et al., 1988). Many intrusive diabase bodies characterize the area; the most prominent occurrence is the Ponta Grossa dike swarm. These dikes trend mainly in the NW direction and some are several tens of meters thick (Almeida, 1986). Compositionally, the dikes are mostly basic, but intermediate and acidic types are also present. The basic dikes generally show Ti content between 2 and 3%, like the extrusive rocks of the NPMP (Piccirillo et al., 1990).

On the northeastern border of the PMP, abundant sills intrude the Late Paleozoic sedimentary column, and, to a lesser extent, the Jurassic/Cretaceous layers (Melfi and Girardi, 1963; Davino et al., 1982). These rocks are compositionally like the volcanic rocks of the NPMP with Ti > 2% (Bellieni et al., 1984; Piccirillo et al., 1988; Ernesto et al., 1999). However, some geochemical differences make possible a distinction of the intrusive bodies. Following the classification of Peate et al. (1992), the Paranapanema magma type occurs at the base of the Paleozoic sequence near the city of Campinas, State of São Paulo. In contrast, the Pitanga Type intrudes the youngest Paleozoic sedimentary rocks, and the Mesozoic rocks (Machado, 2005). In the northeastern portion, rocks are of the Urubici type, and differ from the southern part, indicating

Table 1
Paleomagnetic results for the north PMP sub-province.

Site	Long (°)	Lat (°)	Type	N	Dec (°)	Inc (°)	α_{95} (°)	k	P-Long (°)	P-Lat (°)
East of the Parana River										
KS770	−49.38	−17.96	flow	3	170.2	33.7	8.4	215	36.4	−80.7
KS790	−49.27	−18.07	flow	3	168.5	20.9	4.8	676	72.7	−76.6
KS789	−49.20	−18.10	flow	3	168.9	15.3	16.0	60	83.1	−75.1
KS765	−48.96	−18.15	flow	3	191.3	−16.6	10.2	148	154.7	−61.2
KS764*	−49.32	−18.19	flow	3	234.4	−59.2	5.1	584	170.4	−12.9
KS793	−49.33	−18.19	flow	3	193.6	−26.4	3.2	1474	154.3	−55.2
KS769	−49.31	−18.40	flow	3	175.6	17.5	8.3	223	105.8	−79.6
KS702	−48.29	−18.83	flow	3	161.4	27.2	10.5	140	52.7	−71.7
KS787	−48.32	−18.88	flow	3	165.1	25.2	5.2	573	61.1	−74.6
KS701	−48.33	−18.88	flow	3	181.5	32.3	11.1	125	178.3	−88.0
KS817	−49.37	−18.91	flow	3	4.4	−13.4	8.1	91	330.7	77.2
KS698	−47.90	−19.70	flow	6	184.4	20.2	7.4	82	157.3	−79.8
BA388	−47.96	−19.73	flow	6	160.9	32.8	4.4	233	44.8	71.8
BA336	−47.96	−19.73	flow	5	158.9	25.6	10.5	54	56.0	−68.9
KS682b	−47.85	−19.89	flow	5	181.1	20.2	5.3	212	138.8	−80.7
KS682a	−47.85	−19.89	flow	3	173.8	59.5	7.5	269	325.4	−68.9
KS681	−47.80	−19.96	flow	3	174.3	33.5	15.0	258	91.8	−85.6
KS616	−47.79	−20.06	flow	3	181.8	19.1	7.6	267	142.1	−79.6
KS617	−47.47	−20.11	flow	3	159.4	19.1	6.5	365	66.8	−67.6
KS618	−47.46	−20.13	flow	4	191.5	16.7	14.0	44	178.0	−74.0
KS816	−48.69	−20.17	flow	3	347.1	−30.1	10.2	5	237.3	77.1
KS784	−47.80	−20.25	flow	3	199.6	−12.7	13.3	88	170.1	−57.1
RV3	−47.50	−23.00	sill	15	169.2	33.9	5.5	50	64.2	−79.0
RV2	−47.50	−23.00	sill	13	165.8	27.1	3.6	137	72.8	−74.0
RV1	−47.60	−23.00	sill	9	350.1	−34.4	4.5	133	244.5	79.9
West of the Parana River										
KS832	−53.18	−17.10	flow	4	7.6	−17.7	5.3	306	350.4	79.1
KS812	−51.90	−17.20	dike	3	8.3	−5.6	3.2	1460	338.4	73.5
KS810	−52.93	−17.37	sill	4	10.7	−8.7	2.9	1023	347.2	73.3
KS756	−52.01	−17.47	sill	3	198.7	9.2	6.4	372	185.0	−67.7
KS831	−53.21	−17.86	flow	4	347.8	−47.5	4.3	455	170.7	74.5
KS823	−51.66	−17.94	sill	4	357.9	6.5	2.7	1126	302.6	68.7
KS755	−51.66	−17.94	sill	4	357.6	7.8	5.4	294	301.9	68.0
KS774	−49.50	−18.31	flow	3	171.1	43.2	14.6	73	359.3	−79.3
KS830	−53.20	−18.54	flow	4	2.0	−45.3	2.9	994	114.6	81.5
KS822	−51.13	−18.56	flow	3	354.9	−9.7	7.6	262	288.2	75.5
KS821	−49.79	−18.93	flow	6	352.3	−17.1	5.9	129	272.9	77.4
KS819b	−49.47	−18.96	flow	4	3.5	−21.4	4.5	421	334.2	81.4
KS819a	−49.47	−18.96	flow	3	185.0	18.3	8.5	213	158.1	−79.3
KS828	−53.03	−19.07	flow	4	181.8	22.2	7.3	160	140.2	−82.3
KS826	−51.69	−19.11	flow	3	341.9	−16.0	9.0	187	247.8	69.3
KS827	−51.70	−19.12	flow	3	348.7	−20.0	3.7	1111	255.6	76.0
KS745	−54.44	−19.88	flow	3	352.0	16.7	4.5	759	289.3	60.5
KS837	−54.86	−20.42	flow	5	348.3	−28.5	5.2	220	238.4	77.7
KS742	−54.86	−20.42	flow	6	351.4	−19.4	6.5	107	265.4	76.7
KS840	−54.78	−20.44	flow	4	357.1	−29.3	6.7	336	274.7	84.5
KS738	−54.78	−20.44	flow	4	359.6	−32.0	5.1	325	298.2	86.9
KS743	−54.90	−20.44	flow	4	349.4	−42.0	8.9	109	192.0	79.5
KS740b	−54.75	−20.46	flow	5	358.7	−33.7	7.9	95	273.8	87.6
KS740a	−54.75	−20.46	flow	7	1.9	−35.6	5.4	126	12.4	88.1
KS839	−54.90	−20.50	flow	4	6.9	−23.1	18.6	25	344.2	79.3
KS841*	−54.67	−20.56	flow	3	279.1	−47.1	4.2	70	124.3	−41.1
KS838	−54.96	−20.56	flow	3	195.3	24.1	10.4	143	188.9	−73.3

Long and Lat are site coordinates; P-Long and P-Lat are VGP coordinates.

different evolutionary processes. On the western side of the NPMP, rare sills intrude the Early Permian layers, and few dikes occur in a restricted area (Machado et al., 2015). To the south of the area, basalts with distinct composition are found; they are classified as Ribeira type and have Ti content lower than <2.3 wt% (Machado et al., 2015). In the western NPMP, Machado et al. (2015) describe the occurrence of peperites generated because of the interaction between the first basalt flows and the sediments, which in some border areas, were wet indicating humid environments.

The central part of the NPMP is covered by the sediments of the Bauru Group of Neocretaceous age (Paula e Silva et al., 2009), which occupy the depression formed along the axis of the basin marked by the Paraná river. This subsidence caused gentle dips of the layers towards the basin axis. Dips of only 1-2° were observed in the south of the area (Janasi et al., 2011). As noted by Fernandes et al. (2018), the basalts have variable attitudes from horizontal to shallow dipping, sometimes accompanying the paleo-relief of the pre-existing dunes.

Despite the vast extent of the NPMP (north of the Rio Piquiri lineament, Fig. 1), outcrops are comparatively scarce due to the monotonous relief and the sediments of the post-magmatism Bauru-Caiuá basin. The most favorable area is the eastern border, which exposes (Ernesto et al., 1999) the sills and rare dikes. In this work, 60 new outcrops were sampled mainly in the north and west parts of the NPMP and included flows and sills (Table 1). The sampling sites are the same described by Machado et al. (2015) as sampling was performed concomitantly. Fig. 1 shows the new sites along with the previously studied sites (Ernesto et al., 1990, 1999). Samples were collected using a gasoline-powered drill and oriented by both magnetic and sun compasses. Samples were prepared into standard cylinders for the paleomagnetic measurements carried out in the Laboratory of Paleomagnetism of the University of São Paulo.

3. Rock magnetism

Most of the rocks under analysis comes from the western NPMP. According to Machado et al. (2015), the prevalent minerals in these rocks are plagioclase, pyroxene (augite and pigeonite), and opaque minerals (magnetite, ilmenite, and sulfides), and about 1.5% of goethite as a secondary mineral.

The high-temperature thermomagnetic curves were obtained in the Argon atmosphere and using a Kappabridge (Agico KLY-4) equipment (Fig. 2). The curves generally drop to zero between 540 and 580 °C (Fig. 2a–c), indicating magnetite as the leading magnetic carrier. However, some samples retained a small percentage of magnetization above 600 °C (Fig. 2d), probably due to hematite. The dehydration of the goethite may originate from this hematite. The inflection on some heating curves at around 300–350 °C suggested the presence of maghemite due to low-temperature oxidation.

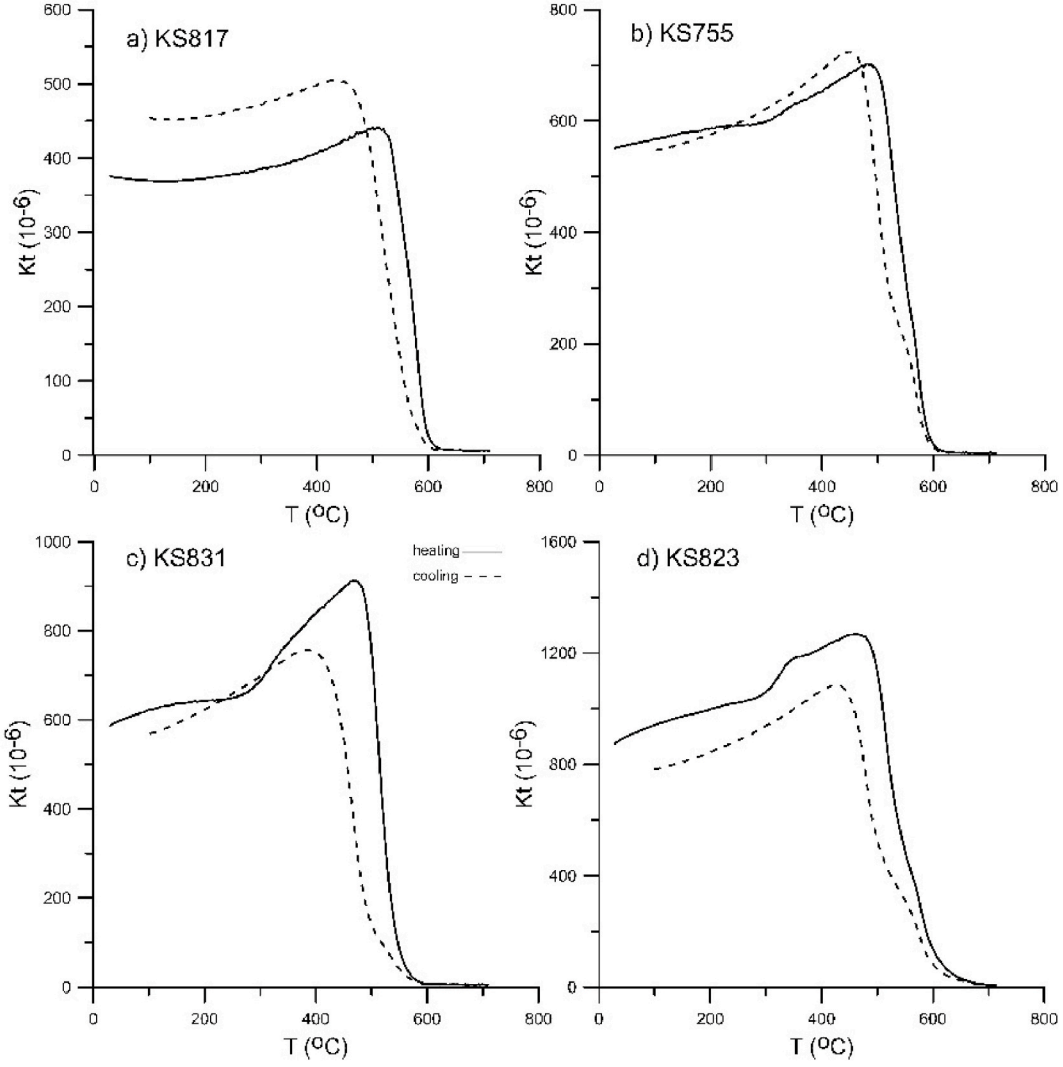

Fig. 2. Thermomagnetic curves showing the susceptibility variation under high temperatures for samples from the north PMP. Solid lines represent the heating curves, and dashed lines are the cooling curves.

The IRM curves (Fig. 3) show saturation of the magnetization at fields lower than 200 mT, compatible with a low coercivity magnetic mineral as magnetite. Hysteresis curves were obtained in a MicroMag 3900 Series VSM (Lake Shore Cryotronics) equipment. The output data gave the relationships MRS/MS (remanence of saturation/saturation magnetization) and HCR/HC (remanent coercive force/coercive force) used in a Day-Dunlop plot (Day et al., 1977; Dunlop, 2002a, b). The results in Fig. 3 indicate that the domain structures of the NPMP samples fall in the pseudo-single domain range, as expected for igneous rocks (Dunlop and Özdemir, 1997). The magnetic minerals in the samples from the eastern NPMP tend to have larger grains (Fig. 3c), as they represent mainly intrusive rocks.

The results from the thermomagnetic curves, IRM acquisition curves, and hysteresis loops indicate that the Ti-poor magnetite is the leading carrier of the magnetization. This mineralogy is similar as that identified in other studies of the PMP rocks (Ernesto et al., 1990, 1996; 1999; Tamrat and Ernesto, 1999; Alva-Valdivia et al., 2003; Goguitchaichvili et al. al., 2013; Mena et al., 2006).

4. Identification of the magnetization components

Samples were subjected to alternating field stepwise AF demagnetizations up to 60–80 mT in a Molspin tumbler demagnetizer, and remanences were measured in a Molspin magnetometer. The routines were performed inside a magnetic-free room. The magnetization components were identified and calculated using the orthogonal diagrams (Zijderveld, 1967) and the Kirschvink (1980) technique (Fig. 4). In general, samples displayed only one stable component of magnetization after the elimination of a soft viscous magnetization at fields up to 15–20 mT. About 10% of the analyzed sites gave no consistent results. The mean magnetization of each sampling site was calculated, giving unit weight to the specimens, and Fisher's (1953) statistics applied (Table 1).

The NPMP rocks display both normal and reversed polarities, which are not homogeneously distributed over the sampling area (Fig. 5a). As already pointed out by Ernesto et al. (1999), on the eastern border, flows and sills of normal polarity concentrate in latitudes higher than 21.5 °S. In contrast, reversed polarity sites dominate in the north (Fig. 5a). This pattern indicates a latitudinal migration of the magmatism. On the other hand, it seems that there is a tendency for rocks of normal polarities to cut the upper sedimentary sequence. Both observations suggest the sills emplaced in few pulses during two brief polarity intervals. This behavior may explain the elongated distribution of the virtual geomagnetic poles (VGPs) calculated for each sampling site (Table 1 and Fig. 6).

The longitudes of the VGPs from sills (Fig. 5b) concentrate in the range 30–90° differing from the other sites (Fig. 5c), which displays a more uniform distribution. This observation suggests that the sills seem to be not independent in time, although intruding different levels of the sedimentary column. Furthermore, the same intrusive body may be overrepresented as the outcrops are discontinuous and challenging to follow laterally. This factor contributes to the elongation of the VGP distribution for the sills and dikes (Fig. 6). In Fig. 6, distribution of VGPs for the intrusive and for the extrusive rocks are elongated in a NE direction, but more accentuated for the sills (Fig. 6a). Both normal and reversed polarity sills (Fig. 6c) follow the same distribution pattern. In contrast, the distributions produced by the data from the SPMP and CPMP are closer to a circular (Fisherian) distribution, which is the predicted distribution by models for the recent geomagnetic field (Tauxe and Kent, 2004).

5. Discussion

The paleomagnetic pole for the NPMP includes the new and old data (Ernesto et al., 1990, 1999) and is located at 84.5°E 82.7°S (N = 128; $A_{95} = 1.8°$; K = 48). For this calculation, sites with less than three results and $\alpha_{95} \geq 15°$ were excluded. Vandamme (1994) cutoff method was

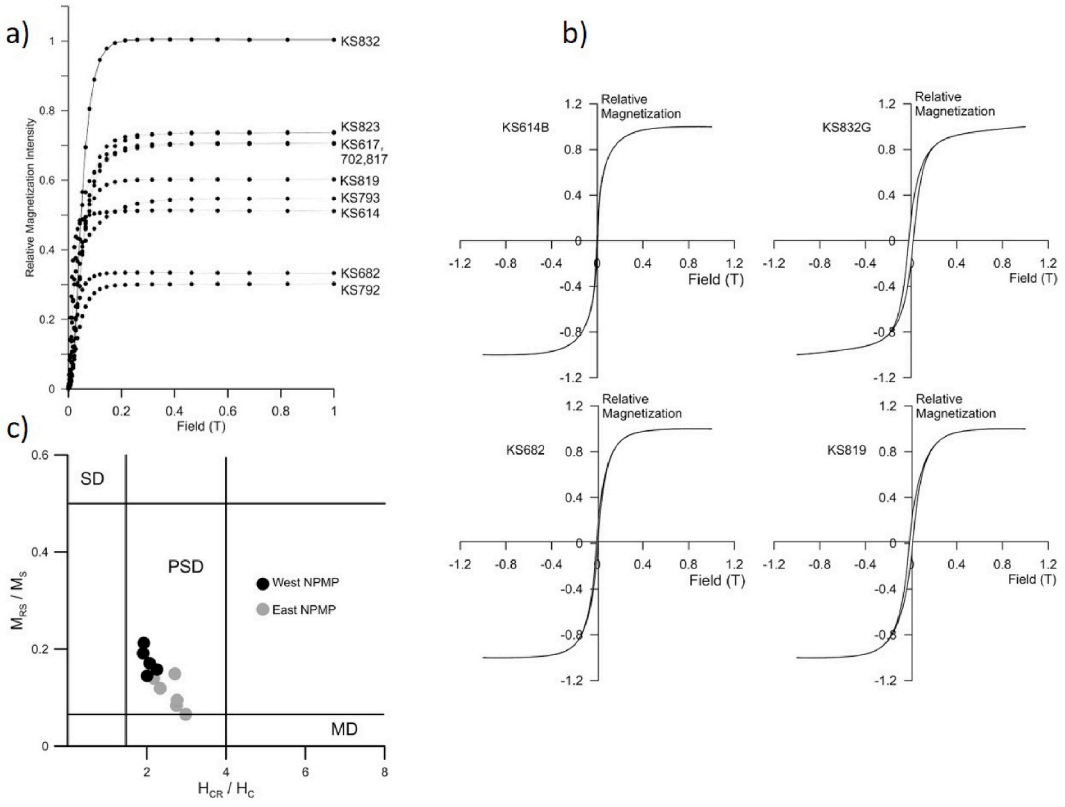

Fig. 3. a) IRM and b) hysteresis curves for some samples of flows and sills; c) Day-Dunlop (Day et al., 1977; Dunlop, 2002a, b) diagram making a distinction between samples from the eastern and western parts of the NPMP.

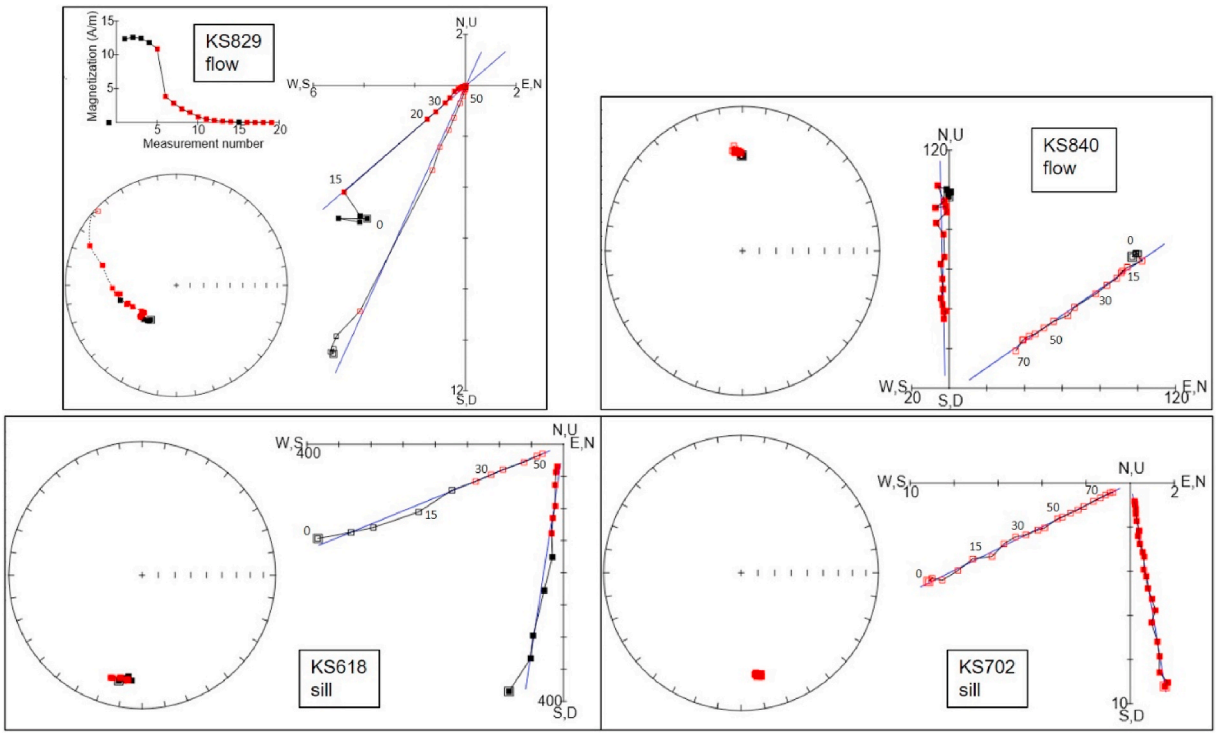

Fig. 4. Orthogonal diagrams for sills and flows and stereographic projections of the magnetization vector during demagnetizations. The variation of the magnetization intensity as a function of the demagnetization steps is shown for sample KS829. Open (full) symbols correspond to negative (positive) inclinations. Blue lines are the adjusted magnetization components through the selected points (red dots). Magnetization units are in 10^2A/m, and field in mT. Plots are according to the PuffinPlot software (Lurcock and Wilson, 2012). (For interpretation of the references to colour in this figure legend, the reader is referred to the Web version of this article.)

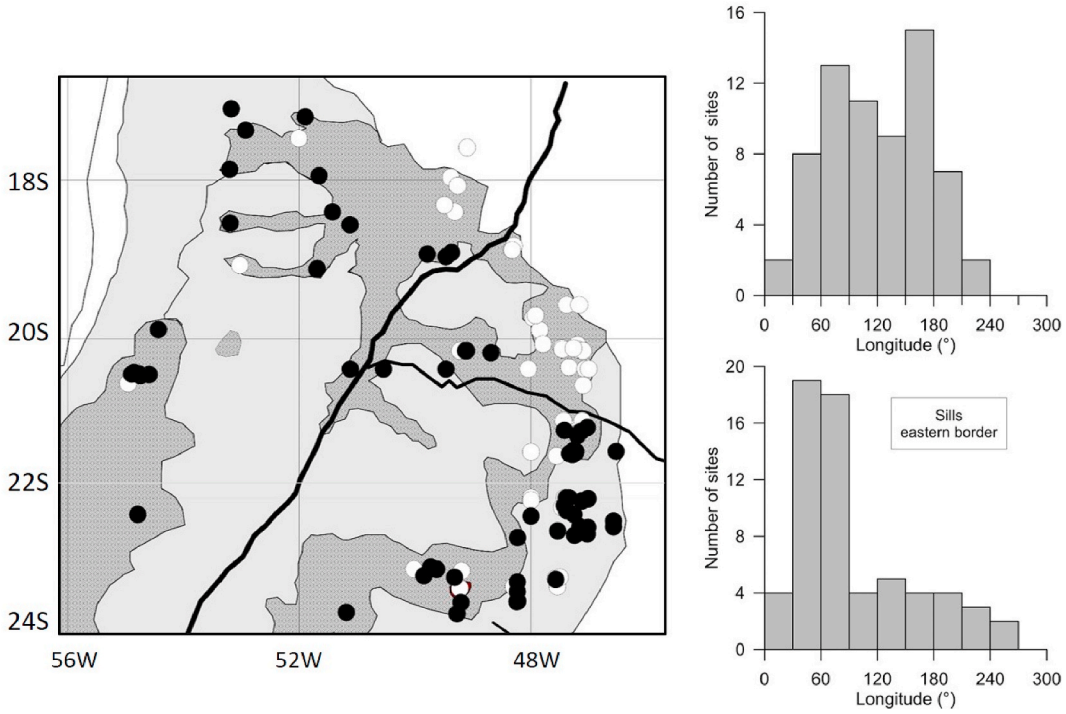

Fig. 5. a) Distribution of the sampling sites according to the remanence polarity: light symbols are normal polarity, and dark symbols are reversed polarity. B) Longitude histograms for the VGPs obtained in this work and b) for the sills from the eastern border.

applied to discard those VGPs that plot far from the main distribution (Fig. 7) and are thought to represent the record of the geomagnetic field during reversals or excursions. However, this pole is affected by the overrepresentation of the sills from the eastern area (data from Ernesto et al., 1999). To minimize the bias, VGPs from close sites, and plotting up to 5° apart were grouped in the same mean result. A new

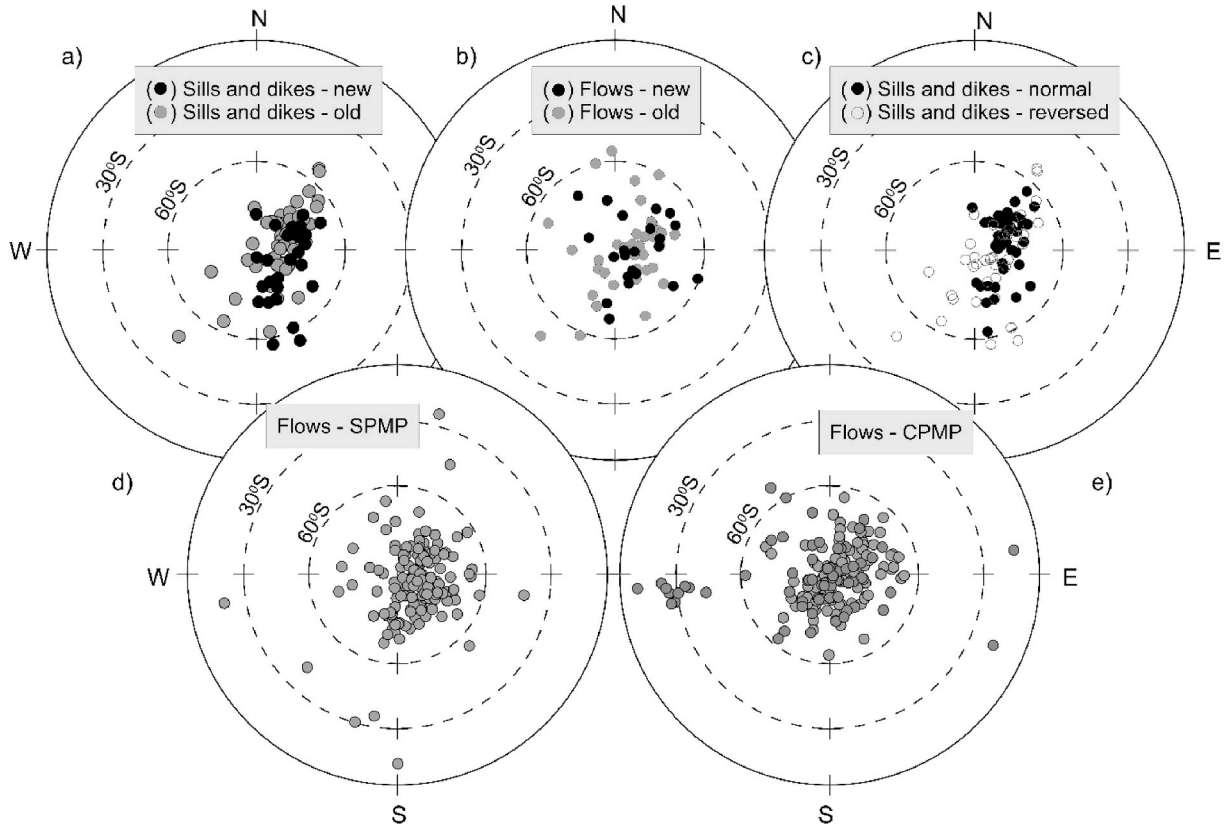

Fig. 6. Distribution of the selected VGPs for the sills and dikes (a) and flows (b) from the NPMP. For comparison, the figure includes the VGPs for the SPMP (d) and CPMP (e). Black symbols are the new data (this work), and gray symbols are the pre-existing data. The distribution of the VGPs for the NPMP intrusive rocks according to their polarity is displayed in (c). All VGPs are south poles on a Wulff projection.

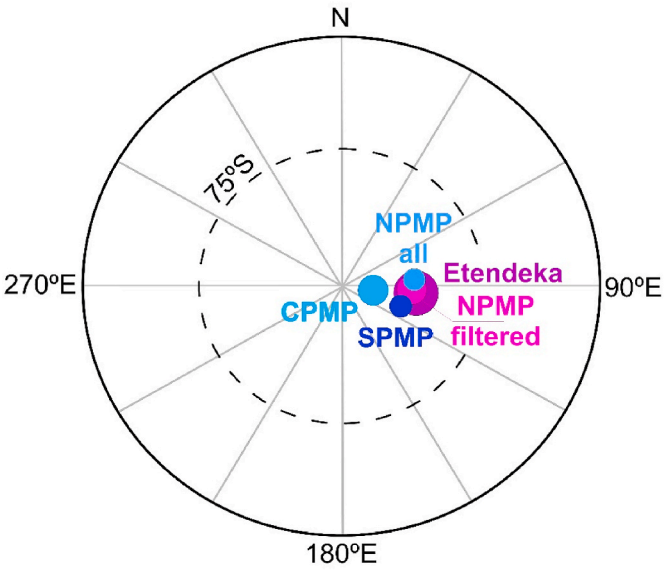

Fig. 7. South hemisphere plot of the paleomagnetic poles from the south (SPMP), central (CPMP), and north (NPMP) Paraná Province (filtered and unfiltered poles). The Etendeka pole (Owen-Smith et al., 2019) is rotated to a pre-drift position using Eagles (2007) parameters.

paleomagnetic pole (NPMP-filtered in Table 2) resulted from 104 sites. This new NPMP pole is compared (Fig. 7) with the SPMP and the CPMP poles, as well as the Etendeka pole (Owen-Smith et al., 2019) after rotation to South America. The NPMP-filtered pole matches well the SPMP and Etendeka poles, with intercepting confidence circles. Given that most of the Paraná magmatism occurred within 1–3 Ma, it is to expect that the paleomagnetic poles statistically coincide as the elapsed time is too brief to allow significant displacement of the South American plate.

However, the CPMP pole is not as close to the other poles as expected. Baksi (2018) reviewed critically all published ages from the PMP and concluded that the reliable estimates of crystallization ages based on Ar/Ar and U-Pb techniques point unequivocally to a maximum of the volcanism at 135-134 Ma, with no noticeable progression south-to-north or west-to-east of the volcanism. Therefore, it seems not plausible to attribute an age difference to the CPMP pole. In fact, U-Pb zircon data for samples from south of the Rio Piquiri Lineament (north limit of the CPMP) indicated a maximum of the volcanic activity in the area between 135.6 ± 1.8 to 134.4 ± 1.1 Ma (Pinto et al., 2011).

The CPMP is the most tectonized area in the province with gentle dips to NW, W, and SW described since the early studies in the PMP (Putzer, 1953). Jacques et al. (2014) defined N–S and E–W fault systems both recently reactivated and affecting the Paraná sedimentary basin and the basement. Furthermore, the area was affected by two meteoritic impacts at about 123 Ma (Crósta et al., 2012, 2010). The Vargeão crater is about 12 km in diameter, and the Vista Alegre is 9.5 km wide. Both seem to be related to fragments of the same impact body affecting the basalts and the underlying Triassic rocks. Although most of the paleomagnetic sampling profiles in the central area seem to be far from the affected areas (Fig. 8), the hydrothermal effects of the impacts may have extended beyond the investigated are (Yokoyama et al., 2015).

The CPMP paleomagnetic pole corresponds to a magnetic direction (Table 2) with a higher inclination than the other PMP-Etendeka poles would produce at a point located at 22°S 52°W. This inclination difference may be corrected for tilting of about 3°-5° in a north-south direction, although the paleo-horizontal was not recognized in the field

Table 2
Paleomagnetic pole for the NPMP based on all site results, and on filtered data, and the poles from SPMP, CPMP, and Etendeka (rotated to South America). Declination, inclination, and paleolatitude produced by these poles to a site at 52°W 22°S.

PMP area	N	Long. (E)	Lat. (S)	A_{95} ()	K	Dec. (°)	Inc. (°)	Paleolat.(°)
NPMP -all sites	128	84.5	82.7	1.8	48	174.8	30.9	16.6
NPMP-filtered	104	93.0	83.0	2.2	40	175.8	30.2	16.2
CPMP	163	105.2	87.7	1.7	45	179.1	35.9	19.9
SPMP	139	109.6	83.8	1.7	51	178.0	30.0	16.1
Etendeka	75	95.7	82.5	3.5	29	175.9	29.2	15.6

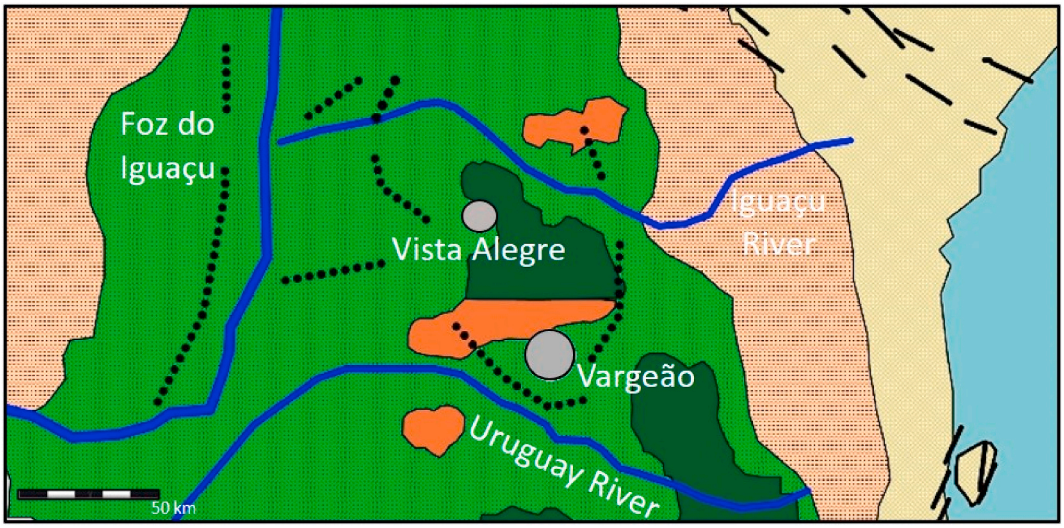

Fig. 8. Location of the impact craters in the CPMP and the relative position of the paleomagnetic sampling sites (black dots) used in this work. Colors same as in Fig. 1. (For interpretation of the references to colour in this figure legend, the reader is referred to the Web version of this article.)

(Alva-Valdivia et al., 2003). A similar correction was proposed to the Ponta Grossa dike swarm (Fig. 1) located in the southern NPMP based on field and magnetometric observations (Ernesto et al., 1999). South America intraplate deformations prior or during the western Gondwana breakup have been considered for some decades (Pindell and Dewey, 1982; Curie, 1984; Unternher et al., 1988; Torsvik et al., 2009; Moulin et al., 2010) to better accommodate the closure of the South Atlantic Ocean in pre-drift reconstructions. Chang et al. (1992) argued that a model involving extension in a NE-SW direction in the area of the NW-SE Ponta Grossa dikes would be sufficient to accommodate differential stretching rates due to the seafloor spreading at the beginning of the breakup process. Moulin et al. (2010) proposed the development of an NW-SE fracture system from ~133 to 130 Ma that practically subdivided the PMP into three sectors. The middle sector roughly corresponds to the CPMP. However, the strike-slip movement along the fractures reaches 150 km at most and seems not enough to account for the needed net variation of almost 3° in latitude. Therefore, some additional structural work is still necessary to ascertain the right correction to apply to the paleomagnetic data, if any.

6. Final remarks

- A high-quality paleomagnetic pole was calculated based on new data from 39 sites of flows and sills from the northern part of the Paraná Magmatic Province (NPMP), and the pre-existing data (Ernesto et., 1990, 1999).
- Data from overrepresented sills were filtered out before the pole calculation as they produce an elongated distribution of VGPs.
- The characteristic magnetizations are of normal and reversed polarities; on the eastern border of the area, polarities follow the same distribution pattern already noticed for the sills (Ernesto et al., 1999), indicating a local north-south migration of the magmatism.
- This new pole matches well the pole for the southern PMP and the Etendela pole, as expected for a short-time-interval of ~1 Myr (Baksi, 2018) for the emplacement of the entire province.
- The paleomagnetic pole for the central PMP differs from the SPMP and NPMP poles, possibly due to intraplate deformation.

Credit author statement

Marcia Ernesto: Conceptualization, Methodology, Data curation, Writing- Reviewing and Editing. Luiz Alberto Zaffani: Formal analysis, Investigation. George Caminha-Maciel: Software, Formal analysis.

Declaration of competing interest

The authors declare that they have no known competing financial interests or personal relationships that could have appeared to influence the work reported in this paper.

Acknowledgments

This work benefits from funding by FAPESP (grant 2004/10081-9 led by L.S. Marques) and CNPq (grant 308475/2015). We are grateful to E. R.V. Rocha-Junior for assistance during fieldwork. Comments by Bernard Henry and another reviewer much helped to improve the text quality.

References

Almeida, F.F.M., 1986. Distribuição regional e relações tectônicas do magmatismo pós–paleozóico no Brasil. Rev. Bras. Geociencias 16, 325–349.
Alva-Valdivia, L.M., Goguitchaichvili, A., Urrutia-Fucugauchi, J., Riisager, J., Riisager, P., Lopes, O.F., 2003. Paleomagnetic poles and paleosecular variation of

basalts from Paraná Magmatic Province, Brazil: geomagnetic and geodynamic implications. Phys. Earth Planet. In. 138, 183–196.
Baksi, A., 2018. Paraná flood basalt volcanism primarily limited to ~1Myr beginning at 135 Ma: new $^{40}Ar/^{39}Ar$ ages for rocks from Rio Grande do Sul, and critical evaluation of published radiometric data. J. Volcanol. Geoth. Res. 355, 66–77.
Bellieni, G., Brotzu, P., Comin-Chiaramonti, P., Ernesto, M., Melfi, A.J., Pacca, I.G., Piccirillo, E.M., 1984. Flood basalt to rhyolite sequences in southern Paraná Plateau (Brazil): petrogenesis, paleomagnetism and geodynamic inferences. J. Petrol. 25, 579–618.
Chang, H.K., Kowsmann, R.O., Figueiredo, A.M.F., Bender, A.A., 1992. Tectonics and stratigraphy of the East Brazil rift system: an overview. Tectonophysics 213, 97–138.
Conceição, J.C., Zalan, P.V., Wolff, S., 1988. Mecanismo, evolução e cronologia do rift Sul-Atlântico. Bol. Geociencias Petrobras 2, 255–265.
Crósta, A.P., Kazzuo-Vieira, C., Pitarello, L., Koeberl, C., Kenkmann, T., 2012. Geology and impact features of Vargeão Dome, southern Brazil. Meteoritics Planet Sci. 47, 51–71.
Crósta, A.P., Doeberl, C., Furuie, R., Kazzuo-Vieira, C., 2010. The first description and confirmation of the Vista Alegre impact structure in the Paraná flood basalts of southern Brazil. Meteoritics Planet Sci. 45, 181–194.
Curie, D., 1984. Ouverture de l'Atlantique sud et discontinuités intra-plaque: une nouvelle analyse. Thesis, Univ. de Bretagne Occidentale, p. 192.
Davino, A., Sinelli, O., Souza, A., Correia, C.T., 1982. Diabásios na região nordeste da Bacia do Paraná. In: XXXII Congresso Brasileiro de Geologia, Proceedings, 4, pp. 1736–1744.
Day, R., Fuller, M., Schmidt, V.A., 1977. Hysteresis properties of titanomagnetites: grain-size and compositional dependence. Phys. Earth Planet. In. 13, 260–267.
Dodd, S.C., Niocaill, C.M., Muxworthy, A.R., 2015. Long duration (> 4Ma) and steady-state volcanic activity in the early Cretaceous Paraná–Etendeka large igneous province: new palaeomagnetic data from Namibia. Earth Planet Sci. Lett. 414, 16–29.
Dunlop, D., 2002a. Theory and application of the Day plot (Mrs/Ms versus Hcr/Hc) 1. Theoretical curves and tests using titanomagnetite data. J. Geophys. Res. 107 (B3), 2056.
Dunlop, D., 2002b. Theory and application of the Day plot (Mrs/Ms versus Hcr/Hc) 2. Application to data for rocks, sediments, and soils. J. Geophys. Res. 107 (B3), 2057.
Dunlop, D., Özdemir, Ö., 1997. Rock Magnetism: Fundamentals and Frontiers. Cambridge University Press, p. 573.
Eagles, G., 2007. New angles on south Atlantic opening. Geophys. J. Int. 168, 353–361.
Ernesto, M., Pacca, I.G., Hiodo, F.Y., Nardy, A.J.R., 1990. Paleomagnetism of the Mesozoic Serra Geral formation, southern Brazil. Phys. Earth Planet. In. 64, 153–175.
Ernesto, M., Comin-Chiaramonti, P., Gomes, C.B., E, M., Castillo, A.M.C., Velazquez, J.C., 1996. Paleomagnetic data from the central Alkaline province, eastern Paraguay. In: Gomes, C.B., Comin-Chiaramonti, P. (Eds.), Alkaline Magmatism in Central-Eastern Paraguay. FAPESP/EDUSP, pp. 85–102.
Ernesto, M., Raposo, M.I.B., Marques, L.S., Renne, P.R., Diogo, L.A., De Min, A., 1999. Paleomagnetism, geochemistry and $^{40}Ar/^{39}Ar$ dating of the northeastern Paraná magmatic province: tectonic implications. J. Geodyn. 28, 321–340.
Fernandes, A.J., Negri, F.A., Sobrinho, J.M.A., Janasi, V.A., 2018. Local geological sections and regional stratigraphy based on physical geology and chemical stratigraphy of the Serra Geral Group from Araraquara to Avaré, SP. Brazil. J. Geol. 48, 243–261.
Fisher, R.A., 1953. Dispersion on a sphere. Proc. Roy. Soc. London Ser. A 217, 295–305.
Goguitchaichvili, A., Cervantes, M.S., Camps, P., Sánchez, L.B., Mena, M., Trindade, R., Aguilar, B.R., Morales, J., Lopez, H.L., 2013. The Earth's magnetic field prior to the Cretaceous Normal Superchron: new palaeomagnetic results from the Alto Paraguay Formation. Int. Geol. Rev. 5, 692–704.
Hartmann, L.A., Baggio, S.B., Bruckmann, M.P., Knijnik, D.B., Lana, C., Massonne, H.-J., Opitz, J., Pinto, V.M., Sato, K., Tassinari, C.C.G., Arena, K.R., 2019. U-Pb geochronology of Parana volcanics combined with trace element geochemistry of the zircon crystals and zircon Hf isotope data. J. South Am. Earth Sci. 89, 219–226.
Jacques, P.D., Salvador, E.D., Machado, R., Grohmann, C.H., Nummer, A.R., 2014. Application of morphometry in neotectonic studies at the eastern edge of the Paraná Basin, Santa Catarina state, Brazil. Geomorphology 213, 13–23.
Janasi, V.A., Freitas, V.A., Heaman, L.H., 2011. The onset of flood basalt volcanism, Northern Paraná Basin, Brazil: a precise U-Pb baddeleyite/zircon age for a Chapecó-type dacite. Earth Planet Sci. Lett. 302, 147–153.
Kirschvink, J.L., 1980. The least-squares line and plane and the analysis of paleomagnetic data. Geophys. J. Roy. Astron. Soc. 62, 699–718.
Lurcock, P.C., Wilson, G.S., 2012. PuffinPlot: a versatile, user-friendly program for paleomagnetic analysis. G-cubed 13, Q06Z45.
Machado, F.B., 2005. Geologia e aspectos petrológicos das rochas intrusivas e efusivas mesozóicas de parte da borda leste da Bacia do Paraná no Estado de São Paulo. M.Sc. monography, UNESP, p. 214.
Machado, F.B., Rocha-Júnior, E.R.V., Marques, L.S., Nardy, A.J.R., 2015. Volcanological aspects of the northwest region of Paraná continental flood basalts (Brazil). Solid Earth 6, 227–241, 2015.
Melfi, A.J., Girardi, V.A.V., 1963. Ocorrência de um sill de diabásio no arenito Botucatu, Município de Igarapava (SP). Boletim Soc. Bras. Geol. II (2), 55–70.
Mena, M., Orgeira, M.J., Lagorio, S., 2006. Paleomagnetism, rock-magnetism and geochemical aspects of early Cretaceous basalts of the Parana magmatic province, Misiones, Argentina. Earth Planets Space 58, 1283–1293.
Milani, E.J., Melo, J.H.G., Souza, P.A., Fernandes, L.A., França, A.B., 2007. Bacia do Paraná. Bol. Geociencias Petrobras 15, 265–287.
Mincato, R.L., Enzweiler, J., Schrank, A., 2003. Novas idades ^{40}Ar-^{39}Ar e implicações na metalogênese dos depósitos de sulfetos magmáticos de Ni-Cu-EGP na Província Ígnea Continental do Paraná. SBGq, Congr. Bras. Geoq. 9, 425–427.
Moulin, M., Aslanian, D., Unternehr, P., 2010. A new starting point for the south and Equatorial Atlantic Ocean. Earth Sci. Rev. 98, 1–37.
Owen-Smith, T.M., Ganerød, M., van Hinsbergen, D.J.J., Gaina, C., Ashwal, L.D., Torsvik, T.H., 2019. Testing early Cretaceous Africa–south America fits with new palaeomagnetic data from the Etendeka magmatic province (Namibia). Tectonophysics 760, 23–36.
Paula e Silva, F., Chang, H.K., Caetano-chang, M.R., 2009. Sedimentation of the Cretaceous Bauru Group in São Paulo, Paraná Basin, Brazil. J. South Am. Earth Sci. 28, 25–39.
Peate, D.W., Hawkesworth, C.J., Mantovani, M.S.M., 1992. Chemical stratigraphy of the Paraná lavas (South America): classification of magma types and their spatial distribution. Bull. Volcanol. 55, 119–139.
Petri, S., Fúlfaro, J.V., 1983. Geologia Do Brasil. T.A. Queiroz e Universidade de São Paulo.
Piccirillo, E.M., Melfi, A.J., 1988. The Mesozoic Flood Volcanism of the Paraná Basin: Petrogenetic and Geophysical Aspects. Instituto Astronômico e Geofísico – Universidade de São Paulo, 600p., São Paulo.
Piccirillo, E.M., Comin-Chiaramonti, P., Melfi, A.J., Stolfa, D., Bellieni, G., Marques, L.S., Giaretta, A., Nardy, A.J.R., Pinese, J.P.P., Raposo, M.I.B., Roisenberg, A., 1988. Petrochemistry of continental flood basalt–rhyolite suites and intrusives from the Paraná Basin (Brazil). In: Piccirillo, E.M., Melfi, A.J. (Eds.), The Mesozoic Flood Volcanism of the Paraná Basin: Petrogenetic and Geophysical Aspects. Instituto Astronômico e Geofísico – Universidade de São Paulo, pp. 107–156.
Piccirillo, E.M., Bellieni, G., Cavazzini, G., Comin-Chiaramonti, P., Petrini, R., Melfi, A.J., Pinese, J.P.P., Zantedeschi, P., De Min, A., 1990. Lower Cretaceous tholeiitic dyke swarm from the Ponta Grossa Arch (southeast Brazil): petrology, Sr-Nd isotopes and genetic relationships with the Paraná flood volcanics. Chem. Geol. 89, 19–48.
Pindell, J., Dewey, J.F., 1982. Permo-Triassic reconstruction of western Pangea and the evolution of the Gulf of Mexico/Caribbean region. Tectonics 1, 179–211.
Pinto, V.M., Hartmann, L.A., Santos, J.O.S., McNaughton, N.J., Wildner, W., 2011. Zircon U–Pb geochronology from the Paraná bimodal volcanic province support a brief eruptive cycle at ~135 Ma. Chem. Geol. 281, 93–102.
Putzer, H., 1953. Diastrofismo "germanótipo" e sua relação com o vulcanismo basáltico na parte meridional de Santa Catarina. Boletim Soc. Bras. Geol. 2, 1953.
Renne, P.R., Ernesto, M., Pacca, I.G., Coe, R.S., Glen, J.M., Prévot, M., Perrin, M., 1992. The age of Paraná flood volcanism, rifting of Gondwanaland, and the Jurassic-Cretaceous boundary. Science 258, 975–979.
Renne, P.R., Deckart, K., Ernesto, M., Féraud, G., Piccirillo, E.M., 1996. Age of the Ponta Grossa dike swarm (Brazil), and implications to Paraná flood volcanism. Earth Planet Sci. Lett. 144, 199–211.
Schetino, A., Scotese, C.R., 2005. Apparent polar wander paths for the major continents (200 Ma to the present day): a palaeomagnetic reference frame for global plate tectonic reconstructions. Geophys. J. Int. 163, 727–759.
Stewart, K., Turner, S., Kelley, S., Hawkesworth, C.J., Kirstein, L., Mantovani, M.S.M., 1996. 3-D 40Ar-39Ar geochronology in the Paraná flood basalt province. Earth Planet Sci. Lett. 143, 95–109.
Tamrat, E., Ernesto, M., 1999. Magnetic fabric and rock-magnetic character of the Mesozoic flood basalts of the Paraná Basin. Brazil. J. Geodyn. 28, 419–437.
Tauxe, L., Kent, D.V., 2004. A simplified statistical model for the geomagnetic field and the detection of shallow bias in paleomagnetic inclinations: was the ancient magnetic field dipolar?. In: Channell, J.E.T., Kent, D.V., Lowrie, W., Meert, J.G. (Eds.), Timescales of the Paleomagnetic Field, vol. 145, pp. 101–115.
Thiede, D.S., Vasconcelos, P.M., 2010. Paraná flood basalts: rapid extrusion hypothesis confirmed by new 40Ar/39Ar results. Geology 38, 747–750.
Torsvik, T.H., Rousse, S., Labails, C., Smethurst, M.A., 2009. A new scheme for the opening of the South Atlantic Ocean and the dissection of an Aptian salt basin. Geophys. J. Int. 177, 1315–1333.
Turner, S., Regelous, M., Kelley, S., Hawkesworth, C., Mantovani, M., 1994. Magmatism and continental breakup in the South Atlantic: high precision ^{40}Ar-^{39}Ar geochronology. Earth Planet Sci. Lett. 121, 333–348.
Unternehr, P., Curie, D., Olivet, J.L., Goslin, J., Beuzart, P., 1988. South Atlantic fits and intraplate boundaries in Africa and south America. Tectonophysics 155, 169–179.
Vandamme, D., 1994. A new method to determine paleosecular variation. Phys. Earth Planet. In. 85, 131–142.
Yokoyama, E., Nédélec, A., Baratoux, D., Trindade, R.I.F., Fabre, S., Berger, G., 2015. Hydrothermal alteration in basalts from Vargeão impact structure, south Brazil, and implications for recognition of impact-induced hydrothermalismon Mars. Icarus 252, 347–365.
Zijderveld, J.D.A., 1967. AC demagnetization of rocks: analysis of results. In: Collinson, D.W., Creer, K.M., Runcorn, S.K. (Eds.), Methods in Paleomagnetism. Elsevier, Amsterdam, pp. 254–286.